

Supplementary Materials for

Impact of expressing cells on glycosylation and glycan of SARS-CoV-2 spike glycoprotein

Yan Wang¹, Zhen Wu², Wenhua Hu³, Piliang Hao⁴, and Shuang Yang^{3*}

¹ Mass Spectrometry Facility, National Institute of Dental and Craniofacial Research, National Institutes of Health, Bethesda, MD 20892, USA

² State Key Laboratory of Genetic Engineering, Department of Biochemistry, School of Life Sciences, Fudan University, Shanghai 200438, China

³ Center for Clinical Mass Spectrometry, Department of Pharmaceutical Analysis, Soochow University, Suzhou, Jiangsu 215123, China

⁴ School of Life Science and Technology, ShanghaiTech University, Shanghai 201210, China

Table S1. List of 98 unique sequence of SARS-CoV-2 spike receptor binding domain. These sequences were extracted from over 20,000 spike glycoproteins (downloaded from GISAID, www.gisaid.org).

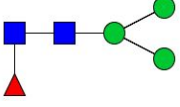
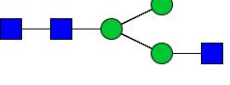
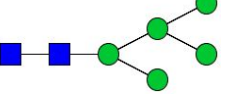
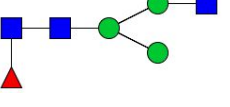
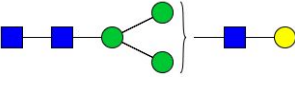
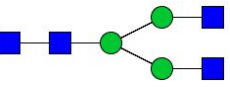
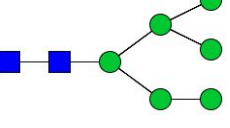
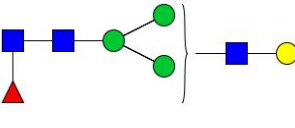
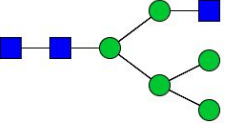
Strain
SARS-CoV-2
2019-12-24 Wuhan/IPBCAMS-WH-01/2019
2020-01-16 Shenzhen/SZTH-004/2020
2020-01-27 India/1-27/2020
2020-01-28 Shanghai/SH0007/2020
2020-02-01 Guangdong/GD2020087-P0008/2020
2020-02-11 Hong Kong/HKPU48-0202/2020
2020-02-19 Hong Kong/HKPU63-1402/2020
2020-02-25 Beijing/BJ1112/2020
2020-02-29 Belgium/BA-02291/2020
2020-02-29 USA/WA-S107/2020
2020-02-29 USA/WA-S106/2020
2020-03-00 USA/AZ-TG268417/2020
2020-03-01 USA/WA-S86/2020
2020-03-02 USA/WA-S32/2020
2020-03-02 USA/WA-S28/2020
2020-03-02 USA/WA-S22/2020
2020-03-02 USA/WA-S23/2020
2020-03-02 USA/WA-S20/2020
2020-03-02 USA/WA-S19/2020
2020-03-03 Finland/FIN03032020A/2020
2020-03-05 USA/WA15-UW11/2020
2020-03-05 USA/WA16-UW12/2020
2020-03-05 USA/WA17-UW13/2020
2020-03-05 France/B2340/2020
2020-03-05 USA/WA-UW40/2020
2020-03-05 USA/WA-S58/2020
2020-03-07 Australia/VIC18/2020
2020-03-08 USA/WA-UW31/2020
2020-03-09 USA/WA-UW68/2020
2020-03-10 USA/WA-UW91/2020
2020-03-11 USA/AZ-TG268905/2020
2020-03-11 Australia/NSW34/2020
2020-03-12 Wales/PHW27/2020
2020-03-12 USA/WA-S140/2020
2020-03-12 USA/WA-S139/2020
2020-03-12 Canada/ON_PHL6980/2020

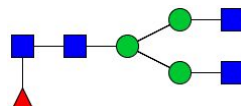
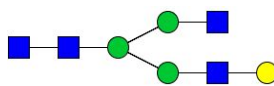
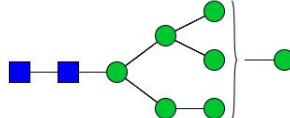
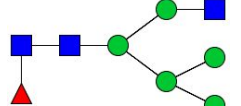
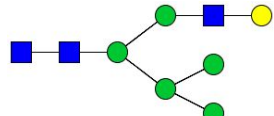
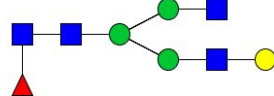
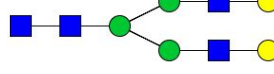
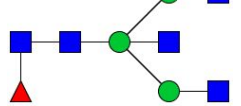
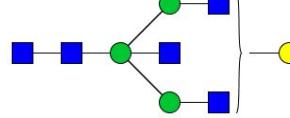
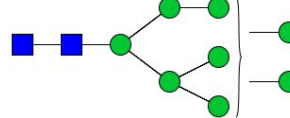
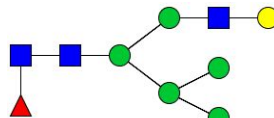
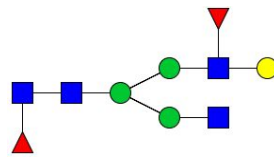
2020-03-13|Scotland/CVR37/2020
2020-03-13|Scotland/CVR42/2020
2020-03-13|USA/WA-S137/2020
2020-03-13|USA/WA-UW204/2020
2020-03-13|USA/WA-NH13/2020
2020-03-14|USA/WA-UW231/2020
2020-03-14|USA/WA-UW270/2020
2020-03-15|USA/WA-UW378/2020
2020-03-15|USA/WA-UW292/2020
2020-03-15|USA/WA-UW286/2020
2020-03-16|Scotland/CVR140/2020
2020-03-16|Scotland/CVR133/2020
2020-03-16|USA/UN-UW-1402/2020
2020-03-16|USA/AZ-TG268002/2020
2020-03-16|USA/WA-UW323/2020
2020-03-16|USA/WA-UW332/2020
2020-03-16|USA/WA-UW338/2020
2020-03-16|USA/UN-UW-1403/2020
2020-03-16|USA/WA-UW244/2020
2020-03-16|USA/WA-UW261/2020
2020-03-17|Australia/VIC329/2020
2020-03-17|USA/AZ-TG268099/2020
2020-03-17|USA/AZ-TG268282/2020
2020-03-17|Australia/VIC149/2020
2020-03-17|USA/WA-S161/2020
2020-03-17|Denmark/ALAB-HH65/2020
2020-03-18|Australia/VIC171/2020
2020-03-19|USA/WA-UW-1587/2020
2020-03-19|USA/WA_0432/2020
2020-03-19|USA/WA-S176/2020
2020-03-19|USA/WA-S221/2020
2020-03-20|USA/AZ-TG271878/2020
2020-03-20|USA/AZ-TG269238/2020
2020-03-20|USA/AZ-TG269358/2020
2020-03-20|England/20144067504/2020
2020-03-21|Scotland/EDB084/2020
2020-03-21|USA/NY-PV09019/2020
2020-03-21|Scotland/CVR375/2020
2020-03-22|Belgium/ULG-9641/2020
2020-03-22|Netherlands/NA_177/2020
2020-03-24|Belgium/HCM-0324151/2020
2020-03-24|USA/WA-S529/2020
2020-03-25|Latvia/0002/2020

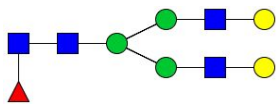
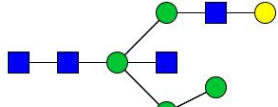
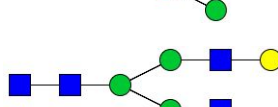
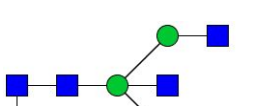
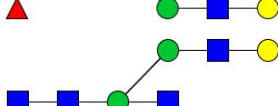
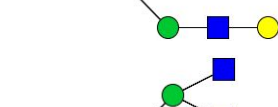
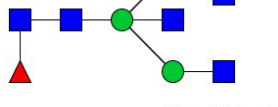
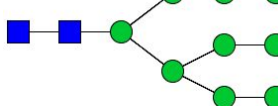
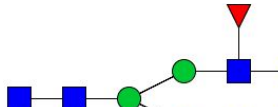
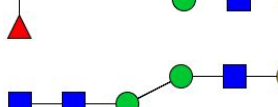
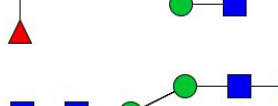
2020-03-26|Russia/Chechenya-83801/2020
2020-03-26|Wales/PHWC-26365/2020
2020-03-27|Australia/VIC662/2020
2020-03-27|Netherlands/NA_238/2020
2020-03-27|USA/TX-HMH0284/2020
2020-03-28|England/CAMB-74650/2020
2020-03-29|England/20140002204/2020
2020-03-30|England/20140064004/2020
2020-03-31|Wales/PHWC-27C5A/2020
2020-03-31|USA/TX-HMH0397/2020
2020-04-01|Wales/PHWC-27CF0/2020
2020-04-03|USA/NY-NYUMC330/2020
2020-04-05|USA/NY-NYUMC287/2020
2020-04-05|England/CAMB-7870E/2020
2020-04-05|USA/WA-S470/2020
2020-04-08|England/CAMB-7AC2B/2020
2020-04-12|Scotland/EDB1424/2020
2020-04-15|England/SHEF-C3CC9/2020

Table S2. Quantitative profiling of N-glycans from SARS-CoV and SARS-CoV-2 expressed in HEK293 cells and baculovirus insect cells. The N-glycans were characterized by a Bruker autoflex MALDI-TOF/TOF-MS. (a) SARS-CoV-2 in HEK293, (b) SARS-CoV-2 in baculovirus insect, (c) SARS-CoV in Baculovirus insect.

(a)

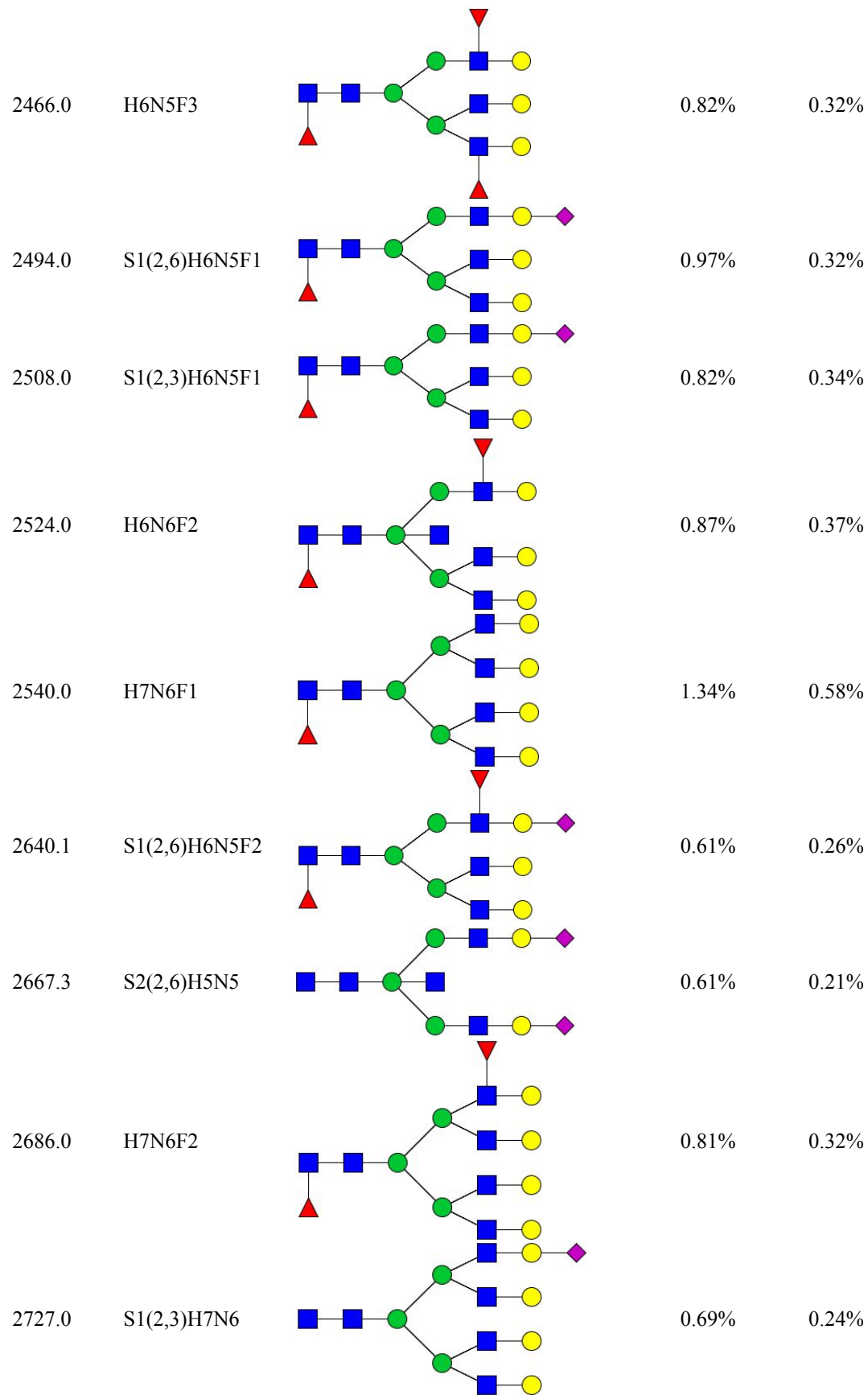
Mass	N-glycan	Composition	Relative Abundance	Standard Deviation
1079.1	H3N2F1		1.86%	0.78%
1136.4	H3N3		1.62%	0.58%
1257.5	H5N2		3.01%	1.30%
1282.5	H3H3F1		1.46%	0.61%
1298.5	H4N3		1.27%	0.55%
1339.5	H3N5		2.93%	1.28%
1419.6	H6N2		1.70%	0.74%
1444.6	H4N3F1		1.32%	0.63%
1460.6	H5N3		1.34%	0.57%

1485.6	H3N4F1		1.51%	0.66%
1501.6	H4N4		1.26%	0.54%
1581.6	H7N2		1.78%	0.71%
1606.6	H5N3F1		1.37%	0.57%
1622.7	H6N3		1.65%	0.67%
1647.7	H4N4F1		1.85%	0.67%
1663.7	H5N4		1.88%	0.82%
1688.7	H3N5F1		1.58%	0.70%
1704.7	H4N5		1.13%	0.47%
1743.7	H8N2		1.58%	0.68%
1768.8	H6N3F1		1.21%	0.54%
1793.8	H4N4F2		1.61%	0.65%

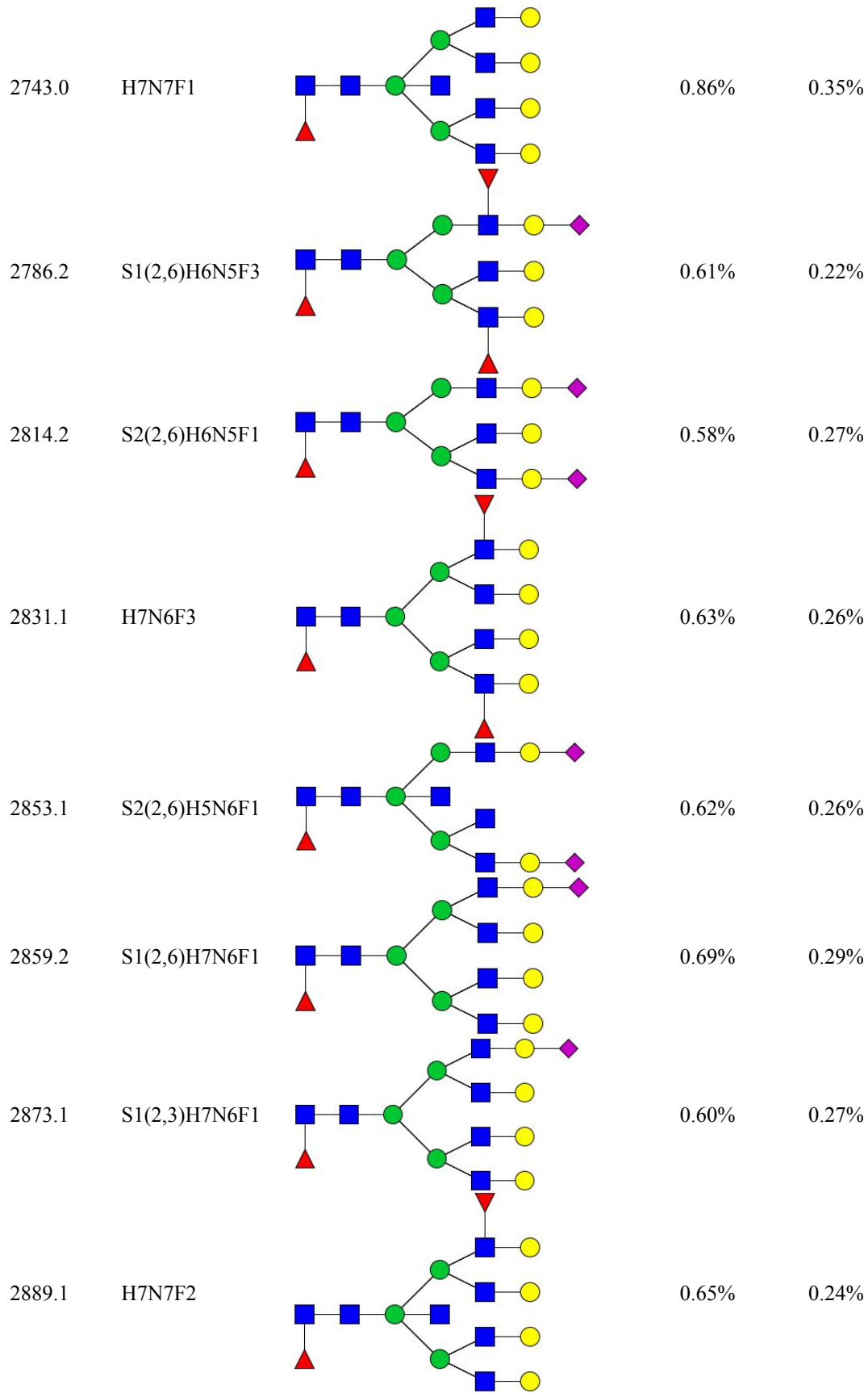
1809.7	H5N4F1		5.49%	2.38%
1825.8	H6N4		1.13%	0.46%
1834.7	S1(2,3)H4N4		1.06%	0.43%
1850.8	H4N5F1		3.26%	1.44%
1866.7	H5N5		1.11%	0.50%
1891.8	H3N6F1		1.15%	0.50%
1905.7	H9N2		1.29%	0.51%
1955.8	H5N4F2		2.77%	1.24%
1967.7	S1(2,6)H4N4F1		2.30%	1.01%
1996.8	S1(2,3)H5N4		4.65%	2.01%
2012.8	H5N5F1		3.42%	1.47%

2028.8	H6N5		1.07%	0.46%
2037.9	S1(2,3)H4N5		1.39%	0.51%
2053.9	H4N6F1		1.03%	0.46%
2100.8	H5N4F3		1.20%	0.57%
2128.8	S1(2,6)H5N4F1		1.82%	0.77%
2142.9	S1(2,3)H5N4F1		2.01%	0.87%
2158.9	H5N5F2		1.33%	0.46%
2174.9	H6N5F1		2.36%	1.03%
2185.9	S1(2,6)H5N5		1.37%	0.59%
2215.9	H5N6F1		1.23%	0.47%
2274.9	S1(2,6)H5N4F2		0.92%	0.38%

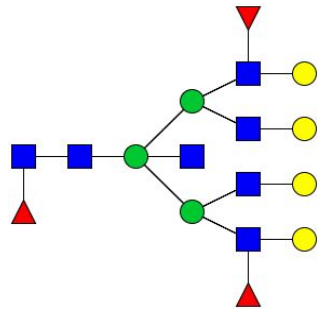
2289.0	S1(2,3)H5N4F2		0.83%	0.33%
2304.9	H5N5F3		0.92%	0.39%
2320.9	H6N5F2		1.16%	0.51%
2330.9	S2(2,3)H5N4		0.48%	0.07%
2332.0	S1(2,6)H5N5F1		0.89%	0.38%
2361.9	S1(2,3)H6N5		1.17%	0.53%
2377.9	H6N6F1		1.36%	0.60%
2402.9	H4N7F2		0.89%	0.17%
2448.2	S2(2,6)H5N4F1		0.71%	0.30%



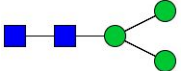
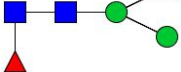
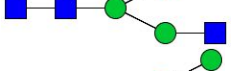




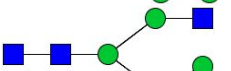
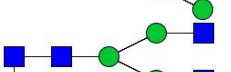
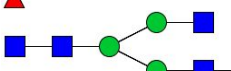
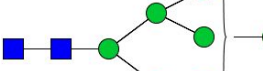

S10

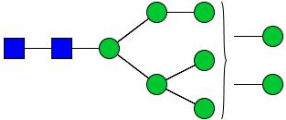
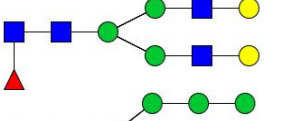
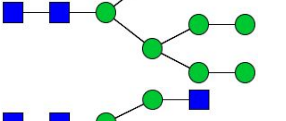
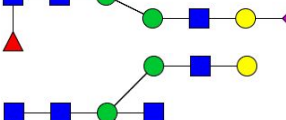
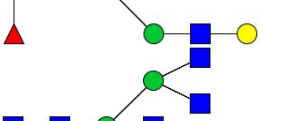
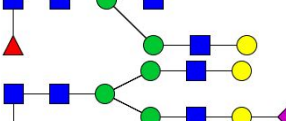
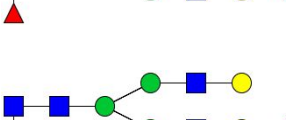
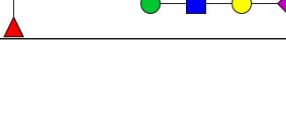


S11

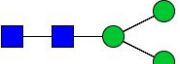
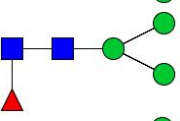
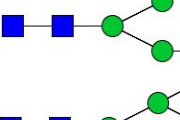
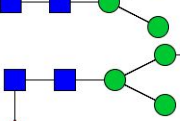
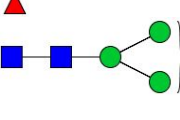

3035.2	H7N7F3		0.50%	0.20%
--------	--------	---	-------	-------

(b)

Mass	N-glycan	Composition	Relative Abundance	Standard Deviation
933.4	H3N2		7.08%	2.44%
1079.5	H3N2F1		18.58%	5.70%
1136.1	H3N3		3.76%	1.54%
1257.6	H5N2		5.47%	1.83%
1282.6	H3H3F1		4.16%	1.70%
1298.3	H4N3		3.21%	1.26%
1339.6	H3N4		6.78%	2.28%
1419.7	H6N2		5.18%	1.83%
1460.7	H5N3		3.12%	1.06%
1485.6	H3N4F1		4.11%	1.51%
1501.5	H4N4		3.06%	1.37%
1581.7	H7N2		5.10%	1.69%

1743.8	H8N2		4.44%	1.35%
1809.6	H5N4F1		2.93%	1.11%
1905.8	H9N2		3.87%	1.35%
1967.8	S1(2,6)H4N4F1		8.39%	2.80%
2012.8	H5N5F1		2.78%	1.02%
2053.7	H4N6F1		2.42%	0.90%
2129.9	S1(2,6)H5N4F1		2.73%	0.87%
2142.9	S1(2,3)H5N4F1		2.83%	1.11%

(c)

N-glycan	Mass	Composition	Relative Abundance	Standard Deviation
H3N2	933.448		12.25%	5.46%
H3N2F1	1079.523		30.80%	14.03%
H3N3	1136.531		4.98%	1.87%
H5N2	1257.687		4.63%	2.16%
H3H3F1	1282.621		4.67%	2.05%
H4N3	1298.584		2.81%	1.28%

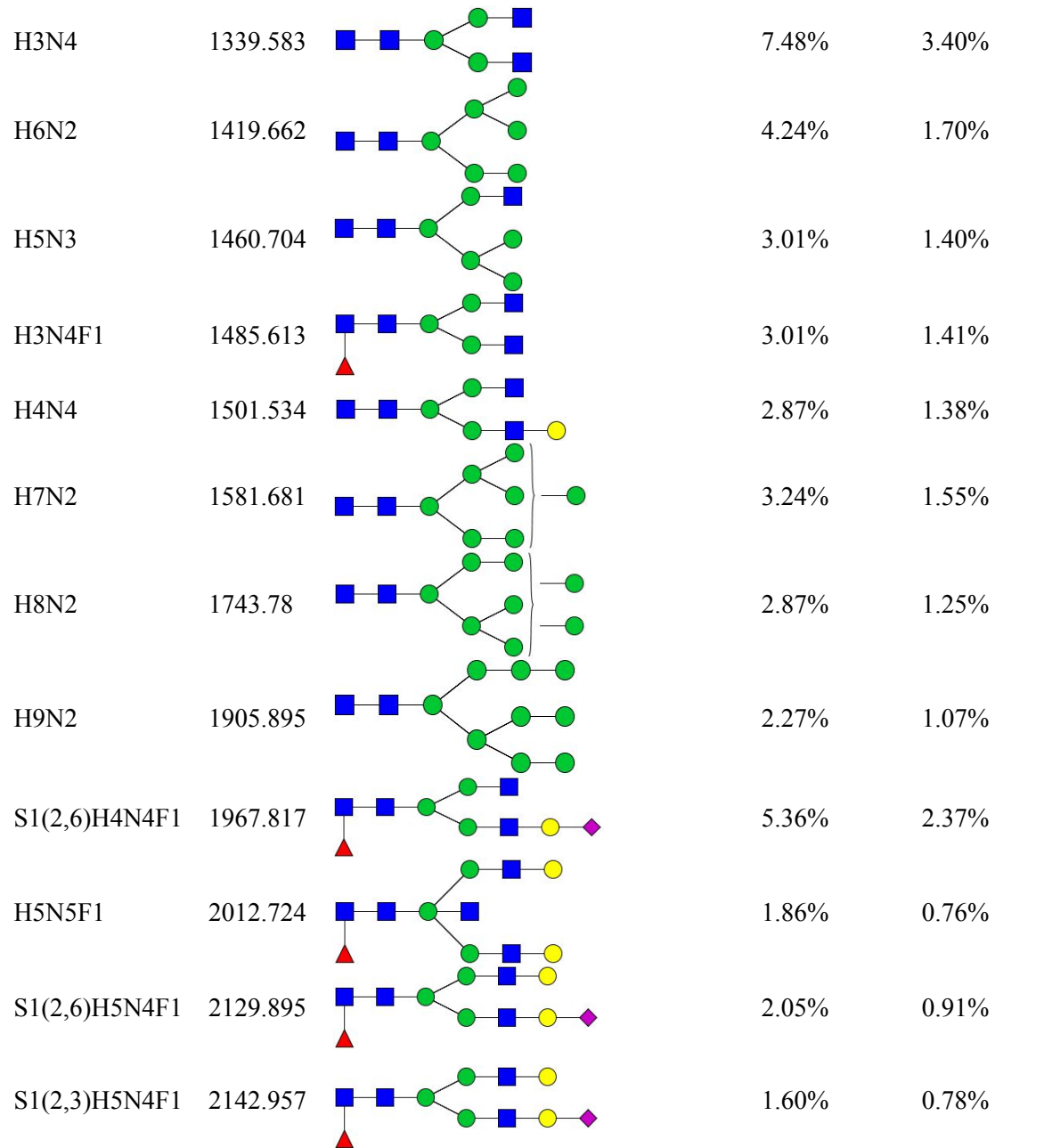


Table S3. O-glycosite prediction based on amino acid sequence of SARS-CoV-2 using ISOglyP. The score < 0.1 sets as “Low”, between 0.1 and 1.5 as “Medium”, and > 1.5 as “High”. Charge is calculated at pH 7.0, assuming D or E as -1, R or K as +1, other amino acids as 0. Note: if the content in the “Detected in our study” is blank indicates not detected.

O-glycosite	O-glycopeptide	Score	Remark	Charge	Detected in our study
S[12]	LLPLVSSQCVN	1.1920	Medium	0	
S[13]	LPLVSSQCVNL	0.6588	Medium	0	
T[19]	QCVNLTTRTQL	1.0946	Medium	1	
T[20]	CVNLTTRTQLP	1.1101	Medium	1	
T[22]	NLTTRTQLPPA	3.4187	High	1	Yes
T[29]	LPPAYTNSFTR	0.6135	Medium	1	Yes
S[31]	PAYTNSFTRGV	0.0909	Low	1	Yes
T[33]	YTNSFTRGVYY	2.3044	High	1	Yes
S[45]	DKVFRSSVLHS	0.1990	Medium	0	
S[46]	KVFRSSVLHST	0.1733	Medium	2	
S[50]	SSVLHSTQDLF	0.1762	Medium	-1	Yes
T[51]	SVLHSTQDLFL	0.7108	Medium	-1	Yes
S[60]	FLPFFSNVTWF	0.2802	Medium	0	
T[63]	FFSNVTWFHAI	0.9574	Medium	0	
S[71]	HAIHVSNGTNGT	0.6026	Medium	0	Yes
T[73]	IHVSGTNGTKR	2.3116	High	2	Yes
T[76]	SGTNGTKRFDN	1.2737	Medium	1	
S[94]	GVYFASTTEKSN	0.5115	Medium	-1	Yes
T[95]	VYFASTTEKSNI	3.1650	High	0	Yes
S[98]	ASTEKSNIIRG	0.0549	Low	1	Yes
T[108]	GWIFGTTLDISK	1.0208	Medium	0	Yes
T[109]	WIFGTTLDISKT	1.2884	Medium	0	Yes
S[112]	GTTLDISKTQSL	0.0970	Low	0	
T[114]	TLDISKTQSLLI	0.4915	Medium	0	
S[116]	DSKTQSLLIVN	0.0482	Low	0	
T[124]	IVNNAITNVVIK	0.6497	Medium	1	
S[151]	HKNNKSWMESE	0.1139	Medium	0	
S[155]	KSWMESEFRVY	0.0627	Low	0	
S[161]	EFRVYSSANNC	0.8680	Medium	0	
S[162]	FRVYSSANNCT	0.3894	Medium	1	
T[167]	SANNCTFEYVS	0.5920	Medium	-1	
S[172]	TFEYVSQPFLM	0.7019	Medium	-1	
S[205]	YFKIYSKHTPI	0.1869	Medium	2	
T[208]	IYSKHTPINLV	0.5399	Medium	1	

S[221]	LPQGFSALEPL	0.1844	Medium	-1	
T[236]	IGINITRFQTL	1.4318	Medium	1	
T[240]	ITRFQTLLALH	0.3274	Medium	1	
S[247]	LALHRSYLTPG	0.0677	Low	1	Yes
T[250]	HRSYLTPGDSS	3.5902	High	0	Yes
S[254]	LTPGDSSSGWT	1.2752	Medium	-1	Yes
S[255]	TPGDSSSGWTA	1.4043	Medium	-1	Yes
S[256]	PGDSSSGWTAG	0.7722	Medium	-1	Yes
T[259]	SSSGWTAGAAA	6.0696	High	0	Yes
T[274]	YLQPRTFLLKY	0.2740	Medium	2	
T[284]	YNENGTITDAV	1.4890	Medium	-2	
T[286]	ENGTITDAVDC	2.7074	High	-3	Yes
S[297]	ALDPLSETKCT	0.2445	Medium	-1	Yes
T[299]	DPLSETKCTLK	0.9730	Medium	1	Yes
T[302]	SETKCTLKSF	0.4250	Medium	1	
S[305]	KCTLKSFVTEK	0.0994	Low	2	
T[307]	TLKSFVTEKGI	0.6810	Medium	1	
T[315]	KGIYQTSNFRV	0.3332	Medium	2	Yes
S[316]	GIYQTSNFRVQ	0.0712	Low	1	Yes
T[323]	FRVQPTESIVR	6.9578	High	1	Yes
S[325]	VQPTESIVRFP	0.1755	Medium	0	Yes
T[333]	RFPNITNLCPF	0.8002	Medium	1	
T[345]	EVFNATRFASV	0.8321	Medium	0	
S[349]	ATRFASVYAWN	0.4014	Medium	1	Yes
S[359]	NRKRISNCVAD	0.2025	Medium	2	Yes
S[366]	CVADYSVLYNS	0.4507	Medium	-1	Yes
S[371]	SVLYNSASFST	0.2287	Medium	0	Yes
S[373]	LYNSASFSTFK	0.4814	Medium	1	
S[375]	NSASFSTFKCY	0.1546	Medium	1	Yes
T[376]	SASFSTFKCYG	0.6416	Medium	1	Yes
S[383]	KCYGVSPTKLN	1.6796	Medium	2	
T[385]	YGVSPTKLNDL	1.9215	Medium	0	
T[393]	NDLCFTNVYAD	0.7760	Medium	-2	
S[399]	NVYADSFVIRG	0.1311	Medium	-2	
T[415]	IAPGQTGKIAD	0.5828	Medium	0	
T[430]	LPDDFTGCVIA	1.5743	Medium	-2	Yes
S[438]	VIAWNSNNLDS	0.0571	Low	-1	Yes
S[443]	SNNLDSKVGGN	0.1871	Medium	0	Yes
S[459]	RLFRKSNLKPF	0.0296	Low	4	
S[469]	FERDISTEIIYQ	0.1938	Medium	-2	Yes
T[470]	ERDISTEIIYQA	2.4744	High	-2	Yes
S[477]	IYQAGSTPCNG	1.0391	Medium	0	Yes
T[478]	YQAGSTPCNGV	3.9641	High	0	Yes

S[494]	YFPLQ S YGFQP	0.1411	Medium	0	Yes
T[500]	YGFQP T NGVGY	3.3049	High	0	Yes
S[514]	RVVVL S FELLH	0.0490	Low	0	
T[523]	LHAP A TVCGPK	3.4564	High	1	Yes
S[530]	CGPK K STNLVK	0.0640	Low	3	
T[531]	GPK K STNLVKN	0.2080	Medium	3	
T[547]	NFNG L TGTGVL	1.0657	Medium	0	Yes
T[549]	NGL T GTGVLTE	1.0029	Medium	-1	Yes
T[553]	GTG V L T ESNKK	0.6164	Medium	1	Yes
S[555]	G V L T ESNKKFL	0.0687	Low	1	Yes
T[572]	RDI A D T TD A VR	2.4076	High	-3	Yes
T[573]	DI A D T TD A VRD	2.2810	High	-3	Yes
T[581]	VRDP Q TLEILD	0.7893	Medium	-2	Yes
T[588]	EILD I T P CSFG	7.1238	High	-2	
S[591]	DIT P C S FGGVS	0.4761	Medium	-1	Yes
S[596]	SFG G V S VITPG	1.0307	Medium	0	
T[599]	G V S V I T PGTNT	6.9243	High	0	Yes
T[602]	VIT P G T NTSNQ	1.1711	Medium	0	
T[604]	TPG T NTSNQVA	0.4224	Medium	0	
S[605]	PG T NT S NQVAV	0.1877	Medium	0	
T[618]	QDV N C T EV P V A	4.2140	High	-1	
T[630]	H A D Q L T PTWRV	3.3027	High	1	Yes
T[632]	D Q L T PTWRVYS	2.8662	High	2	Yes
S[637]	TWR V Y S TGSNV	0.8525	Medium	1	Yes
T[638]	WR V Y S TGSNVF	1.4816	Medium	1	Yes
S[640]	VY S T G SNVFQT	0.1835	Medium	0	Yes
T[645]	SN V F Q TRAGCL	1.5858	Medium	1	Yes
S[659]	EHV N N S YECDI	0.2044	Medium	-3	
S[673]	AGI C A S YQTQT	0.3376	Medium	0	Yes
T[676]	C A S Y Q T QTNSP	0.9560	Medium	0	Yes
T[678]	S Y Q T Q T NSPRR	6.1133	High	2	Yes
S[680]	Q T Q T NS P RRAR	0.5408	Medium	3	Yes
S[686]	PRR A R S VASQS	0.6710	Medium	2	*
S[689]	AR S VASQSIIA	0.8753	Medium	1	*
S[691]	SVASQSII A YT	0.2922	Medium	0	*
T[696]	SI I A Y TMSLGA	0.9601	Medium	0	*
S[698]	I A Y T M S LGAEN	0.3105	Medium	-1	*
S[704]	L G A E NSVAYS N	0.8728	Medium	-1	*
S[708]	NS V A S NN S IA	0.2968	Medium	0	*
S[711]	A S NN S IA I PT	0.3149	Medium	0	*
T[716]	S I A I PT N FTIS	1.0180	Medium	0	*
T[719]	I P T N FTIS V TT	1.8406	Medium	0	*
S[721]	T N FTIS V TT E I	0.5721	Medium	-1	*

T[723]	FTISVTTEILP	1.3194	Medium	-1	*
T[724]	TISVTTEILPV	0.4756	Medium	-1	*
S[730]	EILPVSMTKTS	0.6182	Medium	0	*
T[732]	LPVSMTKTSVD	0.9736	Medium	0	*
T[734]	VSMTKTSVDCT	0.6236	Medium	0	*
S[735]	SMTKTSVDCTM	0.4144	Medium	0	*
T[739]	TSVDCTMYICG	0.7111	Medium	-1	*
S[746]	YICGDSTECNSN	0.3403	Medium	-2	*
T[747]	ICGDSTECNSL	2.2063	High	-2	*
S[750]	DSTECNSLLLQ	0.0613	Low	-2	*
S[758]	LLQYGSFCTQL	0.2721	Medium	0	*
T[761]	YGSFCTQLNRA	0.4619	Medium	1	*
T[768]	LNRALTGIAVE	0.8062	Medium	0	*
T[778]	EQDKNTQEVFA	0.4579	Medium	-2	*
T[791]	KQIYKTPPIKD	2.4684	High	0	*
S[803]	GGFNFSQILPD	0.1008	Medium	-1	*
S[810]	ILPDPSKPSKR	1.0522	Medium	2	*
S[813]	DPSKPSKRSFI	0.4460	Medium	2	*
S[816]	KPSKRSFIEDL	0.0304	Low	1	*
T[827]	LFNKVTLADAG	0.9710	Medium	0	*
T[859]	KFNGLTVLPPL	2.5290	High	1	*
T[866]	LPPLLTDEMIA	0.3977	Medium	-2	*
T[874]	MIAQYTSALLA	1.0765	Medium	0	*
S[875]	IAQYTSALLAG	0.1454	Medium	0	*
T[881]	ALLAGTITSGW	1.8512	Medium	0	*
T[883]	LAGTITSGWTF	2.9975	High	0	*
S[884]	AGTITSGWTFG	0.3768	Medium	0	*
T[887]	ITSGWTFGAGA	1.7742	Medium	0	*
T[912]	NGIGVTQNVLY	1.6318	Medium	0	*
S[929]	ANQFNSAIGKI	0.2422	Medium	1	*
S[937]	GKIQDSLSTA	0.3406	Medium	0	*
S[939]	IQDSLSTASA	0.5543	Medium	-1	*
S[940]	QDSLSTASAL	1.3583	Medium	-1	*
T[941]	DSLSTASALG	3.2324	High	-1	*
S[943]	LSSTASALGKL	0.5452	Medium	1	*
T[961]	AQALNTLVKQL	0.2233	Medium	1	*
S[967]	LVKQLSSNFGA	0.0645	Low	1	*
S[968]	VKQLSSNFGAI	0.1571	Medium	1	*
S[974]	NFGAISSVLND	0.5690	Medium	-1	*
S[975]	FGAISSVLNDI	0.3611	Medium	-1	*
S[982]	LNDILSRLDKV	0.0961	Low	0	*
T[998]	IDRLITGRLQS	0.4928	Medium	1	*
S[1003]	TGRLQSLQTYV	0.1012	Medium	1	*

T[1006]	LQSLQTYVTTQQ	0.5893	Medium	0	*
T[1009]	LQTYVTTQQLIR	1.3446	Medium	1	*
S[1021]	AEIRASANLAA	0.2520	Medium	1	*
T[1027]	ANLAATKMSEC	1.1134	Medium	0	*
S[1030]	AATKMSECVLG	0.1981	Medium	0	*
S[1037]	CVLGQSKRVDF	0.3929	Medium	1	*
S[1051]	GYHLMSFPQSA	0.1247	Medium	0	*
S[1055]	MSFPQSAPHGV	0.3151	Medium	0	*
T[1066]	VFLHVTTYVPAQ	3.6749	High	0	*
T[1076]	QEKNFTTAPAI	6.9229	High	0	*
T[1077]	EKNFTTAPAIC	1.6531	Medium	0	*
S[1097]	EGVVFVSNATHW	0.7228	Medium	-1	*
T[1100]	FVSNATHWFVT	0.4895	Medium	0	*
T[1105]	THWFVTQRNFY	2.6538	High	1	*
T[1116]	EPQIITDNTF	0.7849	Medium	-1	*
T[1117]	PQIITDNTFV	0.6806	Medium	-1	*
T[1120]	ITDNTFVSGN	0.4157	Medium	-1	*
S[1123]	DNTFVSGNCDV	0.3201	Medium	-2	*
T[1136]	GIVNNTVYDPL	0.5617	Medium	-1	*
S[1147]	QPELDSFKEEL	0.0551	Low	-3	*
T[1160]	YFKNHTSPDVD	0.7881	Medium	-1	*
S[1161]	FKNHTSPDVDL	0.7316	Medium	-1	*
S[1170]	DLGDISGINAS	0.1702	Medium	-1	*
S[1175]	SGINASVVNIQ	0.7879	Medium	0	*
S[1196]	KNLNEIDLQ	0.0580	Low	-2	*
T[1231]	AIVMVTIMLCC	1.3899	Medium	0	*
T[1238]	MLCCMTSCCSC	1.8240	Medium	0	*
S[1239]	LCCMTSCCSCSCL	0.4704	Medium	0	*
S[1242]	MTSCCCLKGC	0.1889	Medium	1	*
S[1249]	LKGCCSCGSCC	0.8926	Medium	1	*
S[1252]	CCSCGSCCKFD	0.4318	Medium	0	*
S[1261]	FDEDDSEPVLK	0.3672	Medium	-4	*
T[1273]	VKLHYT	1.2243	Medium	1	*

* These sites belong to S2 domain and did not test in this study.

Table S4. O-glycans for Byonic O-glycopeptide search. O-glycans were prepared by the solid-phase glycan extraction, including β -elimination and permethylation. O-glycans were detected by MALDI-MS. (EDA = ethylene diamine)

List	HEK293	BIC2	BIC1
1	HexNAc(1)	HexNAc(1)	HexNAc(1)
2	HexNAc(1)Hex(1)	HexNAc(1)Hex(1)	HexNAc(1)Hex(1)
3	HexNAc(1)Hex(2)	HexNAc(1)Hex(2)	HexNAc(1)Hex(2)
4	HexNAc(2)Hex(1)	HexNAc(2)Hex(1)	HexNAc(2)Hex(1)
5	HexNAc(1)Hex(2)Fuc(1)	HexNAc(3)Fuc(1)	HexNAc(3)Fuc(1)
6	HexNAc(3)Fuc(1)	HexNAc(2)Hex(1)Fuc(2)	HexNAc(2)Hex(1)Fuc(2)
7	HexNAc(3)Hex(2)NeuAc(1)EDA	HexNAc(3)Hex(2)NeuAc(1) EDA	HexNAc(4)Hex(2)Fuc(2)
8	HexNAc(2)Hex(3)Fuc(1)NeuAc(1)EDA	HexNAc(4)Hex(2)Fuc(2)	HexNAc(3)Hex(4)Fuc(2)
9	HexNAc(4)Hex(2)Fuc(2)	HexNAc(3)Hex(4)Fuc(2)	
10	HexNAc(3)Hex(4)Fuc(2)		

Figure S1. Schematic workflow of spike glycoprotein analysis using protease, MALDI-TOF/TOF-MS and LC-MS/MS. Sialic acid modification was performed by ethyl esterification for α 2,6 linked and ethylene diamine (EDA) amidation for α 2,3 linked sialic acids.

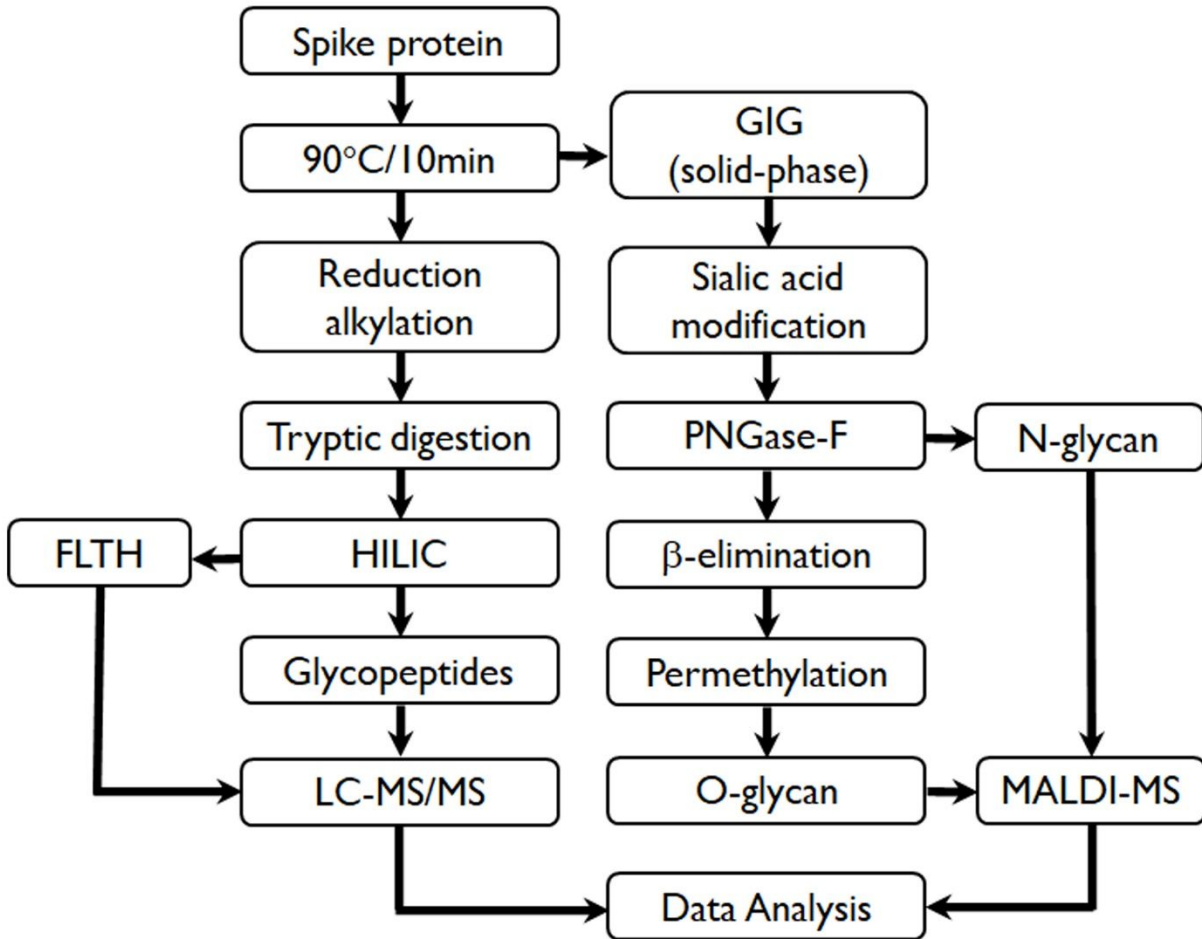


Figure S2. Typical HCD fragmentation of O-glycopeptide precursor, AGCLIGAEHVNNSYECDIPIGAGICASYQTQT[678]NSPR, used for site-specific O-glycosite localization (SARS-CoV-2). The fragments contain one oxonium ion (204.08), one GalGalNAc (365.07), y-ions, and b-ions.

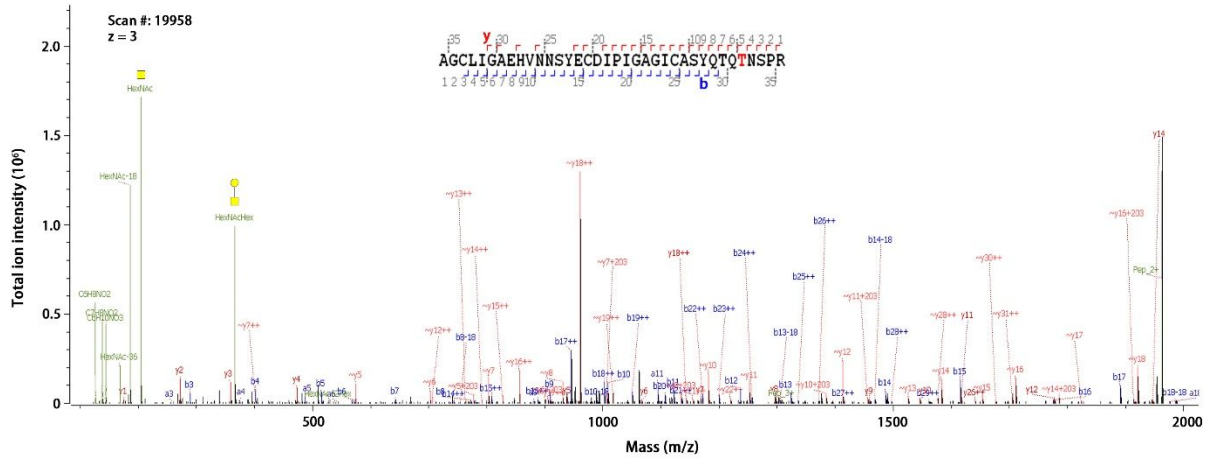


Figure S3. MALDI-MS of O-glycans of SARS-CoV-2 in BIC1, BIC2 and HEK293.

